

## Asymptotic analysis of flame propagation in weakly-strained mixing layers under a reversible chemical reaction

Joel Daou\*

*University of Manchester, School of Mathematics, Manchester, M13 9PL*

*(Received 21 July 2008; final version received 10 November 2008)*

We present an asymptotic study of triple-flames in a strained mixing layer under a reversible reaction, which extends analytical descriptions of these flames beyond the common framework of a single irreversible Arrhenius reaction and constitutes a first step towards accounting for real chemistry effects. The study is carried out in the two-dimensional counterflow configuration and adopts a constant-density assumption along with a generalization of the near-equidiffusional flame (NEF) approximation to the case of a reversible reaction. This generalization involves a convenient and physically motivated distinguished limit comprising a specific scaling of the difference in the activation energies of the forward and backward reactions and of the degree of reversibility. The resulting model yields an extensive set of results for weakly strained triple-flames characterizing the combined influence of the stoichiometry and reversibility of the reaction, the strain rate, and the Lewis numbers of the reactants. The findings include the determination of the local burning speed, temperature and Markstein length along the flame-front, the shape, leading edge and curvature of the latter, and the propagation speed of the triple-flame. In particular, it is found that the Markstein length is affected by the reversibility parameter and the local coordinate along the flame-front whenever the Lewis numbers of the fuel and oxidizer are unequal and is independent of them otherwise; in all cases, however, its value at the leading-edge, which features in the formula derived for the propagation speed, is found to be unaffected by the reversibility. Several features of triple-flames specifically associated with the reversibility of the reaction are described analytically, including the decrease in the propagation speed and flame-front curvature and the increased shift of the location of the leading edge away from the stoichiometric surface with increased reversibility. Some of these features have no counterparts in the irreversible case. For example, whereas the maximum temperature of the triple-flame front occurs at the stoichiometric location in the irreversible case, irrespective of the location of the leading edge, it is typically found to be sandwiched between these two locations in the reversible case.

**Keywords:** Triple-flames; asymptotics; reversible reaction; complex chemistry; partially premixed flames

### 1. Introduction

The importance of triple-flames is now well established in applications involving combustion phenomena such as flame spread over solid or liquid fuel surfaces, flame propagation in mixing layers, ignition and extinction of diffusion flames and flame stabilization in flowing reactive gases. Since early studies on these structures by Phillips [1], Ohki and Tsuge [2] and Dold and collaborators [3,4], several realistic aspects of the problem have been investigated.

---

\*Email: joel.daou@manchester.ac.uk

ISSN: 1364-7830 print / 1741-3559 online

© 2009 Taylor & Francis

DOI: 10.1080/13647830802571085

<http://www.tandf.co.uk/journals>

The investigated aspects include the effect of gas-expansion [5], preferential-diffusion [6,7], unequal temperatures of the fresh reactants [7], the effect of heat-loss [8–11], the stability of these flames [12–14] and others [15, 16]; see the review paper [12] and references therein.

A significant aspect of triple-flame propagation which does not appear to have been investigated in the literature, however, at least as far as analytical studies are concerned, is the sensitivity of triple-flames to chemistry models which go beyond the simplest standard model based on a single irreversible Arrhenius reaction. Although a few numerical investigations have incorporated more realistic and complex chemistry such as in references [17–22], analytical studies of triple-flames corresponding to these more complex models are not available. The aim of this paper is to provide a first step towards accounting analytically for real chemistry effects on triple-flames. To this end, we shall examine the case of a reversible chemical reaction which has been addressed numerically in a recent publication [22]. In this publication, we announced that a related analytical study is to follow, and this is the subject of the present paper.

To motivate our study, we note that the reversibility of the chemical reactions is an important realistic aspect of combustion phenomena, since, for both elementary and global reactions, the reversibility is the rule rather than the exception. Accounting for this aspect is particularly significant for the burning of high caloric fuels, such as hydrogen with oxygen, where the neglect of the dissociation of the products typically leads to unrealistically large values of the flame temperature [23, p. 25]. The importance of reversibility has been well recognized both in *unpremixed combustion*, leading to the broadening of the reaction zone of the diffusion flames among other effects [24–27], as well as in *premixed combustion* [28–31]. The present study will extend such investigations on the effect of reversibility to the context of *partially-premixed combustion* epitomized by triple-flames. To incorporate this effect in the simplest way, we shall consider the case of a single reversible reaction, whose forward and backward rates follow an Arrhenius law.

The paper is structured as follows. We begin by formulating the problem in the context of a thermo-diffusive approximation and reversible reaction, and extract a model in the limit of large activation energy of the forward reaction complete with jump conditions valid at the flame-front of the triple-flame. The precise distinguished limit, including a generalization of the so-called near-equidiffusional flame (NEF) approximation [32, p. 33] and an appropriate scaling of the additional parameters introduced by the reversible nature of the reaction, will be described. The resulting model will then be solved analytically for weak values of the strain rate. The findings will then be presented and discussed in order to clarify the combined influence of the stoichiometry and reversibility of the chemical reaction, the strain rate and the Lewis numbers of the reactants on various characteristics of triple-flame, notably its propagation speed.

## 2. Formulation

The study is carried out in the two-dimensional counterflow configuration, shown in Figure 1, representing an upper stream carrying the oxidizer impinging against a lower stream carrying the fuel. The flow components in the  $X$ ,  $Y$  and  $Z$  directions are given by  $v_X = 0$ ,  $v_Y = -aY$  and  $v_Z = aZ$ , respectively, where  $a$  is the strain rate of the flow. In this configuration, we shall address, within the thermo-diffusive approximation of constant density and constant transport properties, the steady propagation of triple-flames in the mixing layer along the  $X$ -axis; the propagation speed  $\dot{U}$  of the triple-flame is positive if the front is moving along the negative  $X$ -direction.

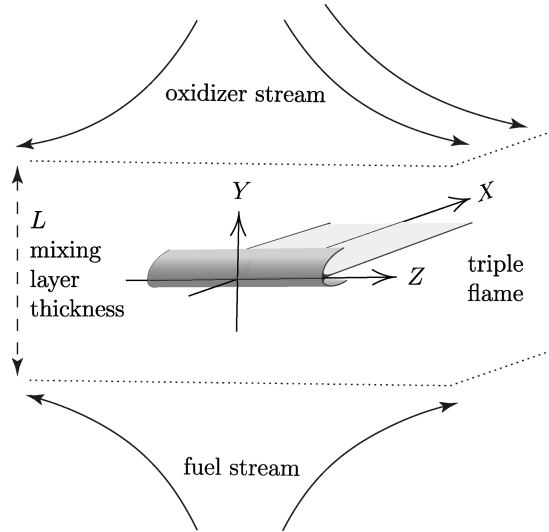
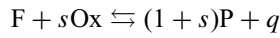


Figure 1. Schematic illustration of a triple-flame in a counterflow configuration.

To account for the reversibility of the chemistry in the simplest way, we consider a single reversible reaction of the form



where  $F$  denotes the fuel,  $Ox$  the oxidizer and  $P$  the product. The quantities  $s$  and  $q$  represent the mass of oxidizer consumed and the heat released per unit mass of fuel. The reaction rate,  $\hat{\omega}$ , is assumed to follow an Arrhenius law in the forward and backward directions of the form

$$\hat{\omega} = B\rho^2 Y_F Y_O \exp\left(-\frac{E}{RT}\right) - B'\rho Y_P \exp\left(-\frac{E'}{RT}\right).$$

Here  $B$  and  $E$  represent the pre-exponential factor and activation energy of the forward reaction,  $B'$  and  $E'$  the pre-exponential factor and activation energy of the backward reaction, and  $\rho$ ,  $Y_F$ ,  $Y_O$  and  $Y_P$  are the density and the mass fractions of the fuel, oxidizer, and product, respectively.

In a frame attached to the flame, the governing equations are

$$\hat{U} \frac{\partial T}{\partial X} - aY \frac{\partial T}{\partial Y} = D_T \left( \frac{\partial^2 T}{\partial X^2} + \frac{\partial^2 T}{\partial Y^2} \right) + \frac{q}{c_p} \frac{\hat{\omega}}{\rho} \quad (1)$$

$$\hat{U} \frac{\partial Y_F}{\partial X} - aY \frac{\partial Y_F}{\partial Y} = D_F \left( \frac{\partial^2 Y_F}{\partial X^2} + \frac{\partial^2 Y_F}{\partial Y^2} \right) - \frac{\hat{\omega}}{\rho} \quad (2)$$

$$\hat{U} \frac{\partial Y_O}{\partial X} - aY \frac{\partial Y_O}{\partial Y} = D_O \left( \frac{\partial^2 Y_O}{\partial X^2} + \frac{\partial^2 Y_O}{\partial Y^2} \right) - s \frac{\hat{\omega}}{\rho} \quad (3)$$

$$\hat{U} \frac{\partial Y_P}{\partial X} - aY \frac{\partial Y_P}{\partial Y} = D_P \left( \frac{\partial^2 Y_P}{\partial X^2} + \frac{\partial^2 Y_P}{\partial Y^2} \right) + (1 + s) \frac{\hat{\omega}}{\rho}. \quad (4)$$

Here,  $D_T$  is the thermal diffusion coefficient and  $D_F$ ,  $D_O$  and  $D_P$  are diffusion coefficients of the fuel, oxidizer and product, respectively.

The conditions at  $X = -\infty$  correspond to a practically frozen mixture where the profiles depend only on  $Y$ , namely,

$$T = T_0, Y_F = \frac{Y_{F,F}}{2} \left[ 1 - \operatorname{erf} \left( \frac{Y}{\sqrt{2D_F/a}} \right) \right], Y_O = \frac{Y_{O,O}}{2} \left[ 1 + \operatorname{erf} \left( \frac{Y}{\sqrt{2D_O/a}} \right) \right],$$

$$Y_P = 0. \quad (5)$$

Here,  $Y_{F,F}$  is the fuel mass fraction in the fuel stream, and  $Y_{O,O}$  is oxidizer mass fraction in the oxidizer stream, and these were used in the boundary conditions, at  $|Y| \rightarrow \infty$  and  $X \rightarrow -\infty$  to obtain (5), and must be used at  $|Y| \rightarrow \infty$  for all  $X$ . Downstream, for  $X \rightarrow \infty$ , the solution are again independent of  $X$ , corresponding to the one-dimensional strong burning solution of the strained diffusion flame.

The non-dimensional formulation of the problem largely follows [7], with the scaled dependent variables being defined by

$$y_F = \frac{Y_F}{Y_{F,st}}, \quad y_O = \frac{Y_O}{Y_{O,st}}, \quad y_P = \frac{Y_P}{(1+s)Y_{F,st}} \quad \text{and} \quad \theta = \frac{T - T_0}{T_{ad} - T_0}.$$

Here the subscript  $st$  refers to values at  $(X = -\infty, Y = Y_{st})$  where  $Y_{st}$  is the location of the upstream stoichiometric surface defined by  $Y_O = sY_F$ , so that, on using (5), we have

$$\operatorname{Serf} \left( \frac{Y_{st}}{\sqrt{2D_F/a}} \right) + \operatorname{erf} \left( \frac{Y_{st}}{\sqrt{2D_O/a}} \right) = S - 1, \quad (6)$$

$$Y_{F,st} = \frac{Y_{F,F}}{S+1} \quad \text{and} \quad Y_{O,st} = \frac{SY_{O,O}}{S+1}, \quad (7)$$

where  $S \equiv sY_{F,F}/Y_{O,O}$  is the normalized stoichiometric coefficient. The quantity  $T_{ad}$  is defined by  $T_{ad} \equiv T_0 + qY_{F,st}/c_p$ , and corresponds to the adiabatic flame temperature under stoichiometric conditions and irreversible reaction.

As unit length, we select  $L/\beta$ , where  $L \equiv \{2D_T/a\}^{1/2}$  is the (thermal) mixing layer thickness and  $\beta \equiv E(T_{ad} - T_0)/RT_{ad}^2$  is the Zeldovich number based on the activation of the forward reaction. As unit speed, we adopt the laminar speed of the stoichiometric equidiffusional planar flame based on the *irreversible* forward reaction in the limit of large  $\beta$ , namely  $S_L^0 = \{4\beta^{-3}Y_{O,st}\rho D_T B \exp(-E/RT_{ad})\}^{1/2}$ .

In terms of the coordinates  $y \equiv \beta(Y - Y_{st})/L$  and  $x \equiv \beta X/L$ , Equations (1)–(3) take the non-dimensional form

$$U \frac{\partial \theta}{\partial x} - \frac{2\epsilon}{\beta} \left( \eta_s + \frac{y}{\beta} \right) \frac{\partial \theta}{\partial y} = \epsilon \left( \frac{\partial^2 \theta}{\partial x^2} + \frac{\partial^2 \theta}{\partial y^2} \right) + \epsilon^{-1} w \quad (8)$$

$$U \frac{\partial y_F}{\partial x} - \frac{2\epsilon}{\beta} \left( \eta_s + \frac{y}{\beta} \right) \frac{\partial y_F}{\partial y} = \frac{\epsilon}{Le_F} \left( \frac{\partial^2 y_F}{\partial x^2} + \frac{\partial^2 y_F}{\partial y^2} \right) - \epsilon^{-1} w \quad (9)$$

$$U \frac{\partial y_O}{\partial x} - \frac{2\epsilon}{\beta} \left( \eta_s + \frac{y}{\beta} \right) \frac{\partial y_O}{\partial y} = \frac{\epsilon}{Le_O} \left( \frac{\partial^2 y_O}{\partial x^2} + \frac{\partial^2 y_O}{\partial y^2} \right) - \epsilon^{-1} w \quad (10)$$

$$U \frac{\partial y_P}{\partial x} - \frac{2\epsilon}{\beta} \left( \eta_s + \frac{y}{\beta} \right) \frac{\partial y_P}{\partial y} = \frac{\epsilon}{Le_P} \left( \frac{\partial^2 y_P}{\partial x^2} + \frac{\partial^2 y_P}{\partial y^2} \right) + \epsilon^{-1} w. \quad (11)$$

Here,  $U = \hat{U}/S_L^0$  is the scaled propagation speed, and

$$\epsilon \equiv \frac{l_{Fl}^0}{L/\beta} = \frac{\beta}{S_L^0} \left( \frac{D_T}{2} \right)^{1/2} a^{1/2},$$

represents a non-dimensional measure of the strain rate (and the typical thickness of the flame relative to its radius of curvature, of order  $L/\beta$ ).  $Le_F \equiv D_T/D_F$ ,  $Le_O \equiv D_T/D_O$  and  $Le_P \equiv D_T/D_P$  are the Lewis numbers of the fuel, oxidizer and product respectively, and  $\eta_s \equiv Y_{st}/\{2D_T/a\}^{1/2}$  is the non-dimensional location of the upstream stoichiometric surface. On account of (5), the latter is given by

$$\text{Serf} \left( \eta_s \sqrt{Le_F} \right) + \text{erf} \left( \eta_s \sqrt{Le_O} \right) = S - 1. \quad (12)$$

In terms of the new variables, the boundary conditions imply that

$$\begin{aligned} \theta &= 0, \\ y_F &= \frac{S+1}{2} \left[ 1 - \text{erf} \left( \left( \eta_s + \frac{y}{\beta} \right) Le_F^{1/2} \right) \right], \\ y_O &= \frac{S+1}{2S} \left[ 1 + \text{erf} \left( \left( \eta_s + \frac{y}{\beta} \right) Le_O^{1/2} \right) \right], \\ y_P &= 0 \qquad \qquad \qquad \text{as } x \rightarrow -\infty \text{ or } y \rightarrow \pm\infty \end{aligned} \quad (13)$$

and

$$\frac{\partial \theta}{\partial x} = \frac{\partial y_F}{\partial x} = \frac{\partial y_O}{\partial x} = \frac{\partial y_P}{\partial x} = 0 \text{ as } x \rightarrow +\infty. \quad (14)$$

The non-dimensional reaction rate  $\omega$  is given by

$$\omega = \frac{\beta^3}{4} \left[ y_F y_O - r y_P \exp \frac{-\alpha \psi}{1 + \alpha(\theta - 1)} \right] \exp \frac{\beta(\theta - 1)}{1 + \alpha(\theta - 1)}, \quad (15)$$

where  $\alpha \equiv (T_{ad} - T_0)/T_{ad}$ , and where

$$r \equiv \frac{B' (Y_{F,F} + S Y_{O,O})(S + 1)}{B \rho Y_{F,F} Y_{O,O} S} \quad \text{and} \quad \psi \equiv \frac{E' - E}{R(T_{ad} - T_0)} \quad (16)$$

are two additional parameters introduced by the reversibility of the reaction;  $r$  is proportional to the ratio of the pre-exponential factors of the backward and forward reactions, and  $\psi$  is the scaled difference of their activation energies. Naturally,  $r$ , which is a main parameter in this study, is zero for an irreversible reaction.

The formulation of the problem is now complete, and is given by Equations (refeq8dtemp)–(15). This eigen-boundary value problem allows, in principle, the deter-

mination of the (scaled) propagation speed  $U$  (an eigenvalue) in terms of the parameters  $\epsilon$ ,  $r$ ,  $S$ ,  $\psi$ ,  $Le_F$ ,  $Le_O$ ,  $Le_P$ ,  $\beta$  and  $\alpha$ . Although this is a rather complicated problem, involving four PDEs, an eigenvalue, and nine parameters, it can be greatly simplified in many circumstances. For example, the common equidiffusional assumption,  $Le_F = Le_O = Le_P = 1$ , implies that  $y_F$  and  $y_O$  can be expressed in terms of  $\theta$ , namely by the right-hand-sides of (13.b) and (13.c) from which  $\theta$  is subtracted, and that  $y_P = \theta$ . It follows that a single equation involving  $\theta$  is needed which, for  $S = 1$  (and thus  $\eta_s = 0$ ), takes the form

$$U \frac{\partial \theta}{\partial x} - \frac{2\epsilon}{\beta^2} y \frac{\partial \theta}{\partial y} = \epsilon \left( \frac{\partial^2 \theta}{\partial x^2} + \frac{\partial^2 \theta}{\partial y^2} \right) + \epsilon^{-1} w$$

with the requirement that

$$\theta = 0 \quad \text{as } x \rightarrow -\infty \text{ or } y \rightarrow \pm\infty, \quad \frac{\partial \theta}{\partial x} = 0 \quad \text{as } x \rightarrow +\infty,$$

and where

$$w = \frac{\beta^3}{4} \left[ (1 - \theta)^2 - \text{erf}^2 \frac{y}{\beta} - r \theta \exp \frac{-\alpha \psi}{1 + \alpha(\theta - 1)} \right] \exp \frac{\beta(\theta - 1)}{1 + \alpha(\theta - 1)}.$$

The equidiffusional problem aforementioned has in fact been tackled numerically in a recent publication [22] for a range of values of  $\epsilon$ ,  $r$  and  $S$ , and fixed values of the other parameters (namely,  $\psi = 1$ ,  $\beta = 8$ , and  $\alpha = 0.85$ ). We announced in [22] that an asymptotic treatment of the problem is to appear in a coming paper. The present paper provides this treatment, carried out in a suitably specified distinguished limit, which will be developed in the next section.

### 3. Asymptotic analysis

#### 3.1. Distinguished limit

In this section, generalizing to the case of a reversible reaction the analysis of triple-flames carried out in [7] for an irreversible reaction, we begin by reformulating the problem in the asymptotic limit  $\beta \rightarrow \infty$  and  $\epsilon \sim 1$ , where  $\beta$  is the Zeldovich number based on the activation energy  $E$  of the forward reaction. In this limit we also assume that the parameter  $\psi$ , the scaled difference of the activation energies  $E'$  and  $E$  defined in (16), is of  $O(1)$ . The latter assumption is motivated by a well known relation between the difference in the activation energies and the enthalpy of the reaction, namely that this difference is equal to the enthalpy, in the case of an elementary reaction [23, p. 20], i.e.  $\psi = 1$  in our notation; since the analysis is not restricted to elementary reactions, we are simply assuming that  $\psi$  is a constant which is independent of the activation energies, since this assumption is more general but consistent with  $\psi = 1$  which should hold for elementary reactions.

Furthermore, we adopt as in [7] the near-equidiffusional approximation for which  $l_F \equiv \beta(Le_F - 1)$  and  $l_O \equiv \beta(Le_O - 1)$  are of order unity; for simplicity we also assume that  $Le_P = 1$  which implies that  $y_P = \theta$  and thus only the three dependent variables  $y_F$ ,  $y_O$ , and  $\theta$  need be considered henceforth. Finally, we scale the reversibility parameter so as to insure that the deviation of temperature in the burnt gas from unity remains of order

$\beta^{-1}$  for  $y \sim 1$ . This is achieved if

$$R \equiv r \beta^2 \exp(-\alpha\psi) \sim 1, \tag{17}$$

meaning that weakly reversible reactions, for which  $r = O(\beta^{-2})$ , are considered.<sup>1</sup> Although other scaling for  $r$  are possible, the present one is sufficient to capture reversibility effects in the simplest way, since, as we shall see, it leads to significant  $O(1)$  variations in the propagation speed for its irreversible value.

In summary, we shall consider the distinguished limit

$$\beta \rightarrow \infty \quad \text{with} \quad \epsilon, \psi, l_F, l_O \text{ and } R \sim 1. \tag{18}$$

This limit is used in the next section to obtain a  $\beta$ -free reformulated problem. In the reformulated problem, we subsequently consider the limit  $\epsilon \rightarrow 0$ . The results to be derived are thus expected to be valid provided the activation energy is large and the strain rate is small, more precisely for  $\beta^{-1} \ll \epsilon \ll 1$ .

### 3.2. A $\beta$ -free reformulated problem

For  $\beta \rightarrow \infty$ , the reaction zone is confined to an infinitely thin region or flame surface given by  $F(x, y) = x - f(y) = 0$ , say. In a coordinate system  $(\xi, y)$  attached to the flame with  $\xi = x - f(y)$ , the Laplacian is given by

$$\Delta = (1 + f'^2) \frac{\partial^2}{\partial \xi^2} + \frac{\partial^2}{\partial y^2} - f'' \frac{\partial}{\partial \xi} - 2f' \frac{\partial}{\partial \xi \partial y} \tag{19}$$

The upstream boundary conditions (13) can be linearized in the limit considered as

$$\theta = 0, \quad y_F = 1 - \frac{\gamma_F}{\beta} y, \quad y_O = 1 + \frac{\gamma_O}{\beta} y, \tag{20}$$

in the flame-front region  $y \sim 1$ . Here  $\gamma_F, \gamma_O$  are given by

$$\gamma_F = \frac{2\exp(-\eta_s^2)}{\sqrt{\pi}(1 - \text{erf}(\eta_s))}, \quad \gamma_O = \frac{2\exp(-\eta_s^2)}{\sqrt{\pi}(1 + \text{erf}(\eta_s))}, \tag{21}$$

and can be readily expressed in terms of  $S$  since within the near-equidiffusional approximation adopted Equation (12) implies that

$$\eta_s = \text{erf}^{-1} \left( \frac{S - 1}{S + 1} \right), \tag{22}$$

---

<sup>1</sup>The consistency of this scaling will become clear after the reaction-zone analysis in Section 3.3 and the results to be derived thereafter. A quick remark here is that this scaling insures that both terms in the square bracket in (15) are  $O(\beta^{-2})$  in the reaction zone with  $y_F, y_O, \theta - 1$  being  $O(\beta^{-1})$  there. Thus, with this scaling of  $r, \omega$  remains  $O(\beta)$  in the reaction zone, as in the irreversible case.

to leading order, and hence

$$\gamma_F = S\gamma_O = (S + 1) \frac{E}{\sqrt{\pi}} \quad \text{where} \quad E \equiv \exp \left[ - \left\{ \operatorname{erf}^{-1} \left( \frac{S - 1}{S + 1} \right) \right\}^2 \right]. \quad (23)$$

We shall use expansions in terms of  $\beta^{-1}$  of the form

$$y_F = y_F^0 + \beta^{-1}y_F^1 + \dots, \quad y_O = y_O^0 + \beta^{-1}y_O^1 + \dots, \quad \theta = \theta^0 + \beta^{-1}\theta^1 + \dots.$$

Then, given that the gradients in the upstream boundary conditions (20) are of order  $\beta^{-1}$ , and that  $r$  is taken to be  $O(\beta^{-2})$ , we have  $\theta^0 + y_F^0 = 1$ ,  $\theta^0 + y_O^0 = 1$ , identically, and

$$\theta^0 = 1, \quad y_F^0 = 0, \quad y_O^0 = 0 \quad \text{in the burnt gas} \quad \xi \geq 0. \quad (24)$$

In terms of  $\theta^0$  and the excess enthalpy  $h \equiv \theta^1 + y_F^1$  and  $k \equiv \theta^1 + y_O^1$ , the governing equations yield

$$U \frac{\partial \theta^0}{\partial \xi} = \epsilon \Delta \theta^0 \quad (25)$$

$$U \frac{\partial h}{\partial \xi} = \epsilon \Delta h + \epsilon l_F \Delta \theta^0 \quad (26)$$

$$U \frac{\partial k}{\partial \xi} = \epsilon \Delta k + \epsilon l_O \Delta \theta^0 \quad (27)$$

where Equations (26) and (27) are valid across the reaction sheet and (25) is only valid for  $\xi \neq 0$ . These equations are to be solved on both sides of the reaction sheet,  $\xi < 0$  and  $\xi > 0$ , with the jump conditions

$$[\theta^0] = [h] = [k] = 0 \quad (28a)$$

$$\left[ \frac{\partial h}{\partial \xi} \right] = -l_F \left[ \frac{\partial \theta^0}{\partial \xi} \right] \quad (28b)$$

$$\left[ \frac{\partial k}{\partial \xi} \right] = -l_O \left[ \frac{\partial \theta^0}{\partial \xi} \right] \quad (28c)$$

$$\epsilon \sqrt{1 + f'^2} \left[ \frac{\partial \theta^0}{\partial \xi} \right] = - \left( 1 + \frac{\sqrt{(h - k)^2 + 4R}}{2} \right)^{1/2} \exp \left( \frac{h + k - \sqrt{(h - k)^2 + 4R}}{4} \right) \quad (28d)$$

at  $\xi = 0$ ; see the next section for a brief justification of these jump conditions. Here and below  $[\varrho] \equiv \varrho(\xi = 0^+, y) - \varrho(\xi = 0^-, y)$  indicates the jump of any quantity  $\varrho$ .

In addition, the upstream boundary conditions, which follow from (20), are

$$\theta^0 = 0, \quad h = -\gamma_F y, \quad k = \gamma_O y \quad \text{as} \quad \xi \rightarrow -\infty. \quad (29)$$

These can also be used for finite  $\xi$  and  $|y| \rightarrow \infty$  since they are exact solutions of (25)–(27). As condition in the burnt gas, we shall simply require that  $\theta^0 = 1$  and that the solutions are free from exponentially growing terms as  $\xi \rightarrow \infty$ .

**3.3. Justification of the jump conditions**

This section is dedicated to a brief derivation of the jump conditions (28), in which only the last condition is seen to depend on the reversibility parameter. The other conditions are identical to those of the irreversible case [7], and their derivation follows exactly the same methodology commonly used in the irreversible case (see e.g. [32, p. 39] and [33, p. 527]). Thus we focus our effort on the derivation of Equation (28d) which deserves more attention. To this end, we introduce a stretched variable  $\bar{\xi}$  and inner expansions in the reaction zone given by

$$\xi = \frac{\bar{\xi}}{\beta}, \quad \theta = 1 + \frac{\Theta^1(\bar{\xi}, y)}{\beta} + \dots, \quad y_F = \frac{F^1(\bar{\xi}, y)}{\beta} + \dots, \quad y_O = \frac{O^1(\bar{\xi}, y)}{\beta} + \dots \tag{30}$$

The reaction term in (15) and the Laplacian in (19) then take the form

$$\omega \sim \frac{\beta}{4} [F^1 O^1 - R] \exp \Theta^1 \quad \text{and} \quad \Delta \sim \beta^2 (1 + f'^2) \frac{\partial^2}{\partial \bar{\xi}^2}$$

provided  $R \equiv r\beta^2 \exp(-\alpha\psi)$  is  $O(1)$  as anticipated. To leading order, the governing equations (8)–(11) thus imply that

$$\begin{aligned} \epsilon^2 (1 + f'^2) \frac{\partial^2 \Theta^1}{\partial \bar{\xi}^2} + \frac{1}{4} [F^1 O^1 - R] \exp \Theta^1 &= 0 \\ \epsilon^2 (1 + f'^2) \frac{\partial^2 F^1}{\partial \bar{\xi}^2} - \frac{1}{4} [F^1 O^1 - R] \exp \Theta^1 &= 0 \\ \epsilon^2 (1 + f'^2) \frac{\partial^2 O^1}{\partial \bar{\xi}^2} - \frac{1}{4} [F^1 O^1 - R] \exp \Theta^1 &= 0, \end{aligned}$$

within the distinguished limit (18). These equations can be reduced to a single one, since  $F^1$  and  $O^1$  can be expressed in terms of  $\Theta^1$  by  $F^1 = h^+ - \Theta^1$  and  $O^1 = k^+ - \Theta^1$ , where  $h^+ \equiv (\theta^1 + y_F^1)|_{\xi=0+}$  and  $k^+ \equiv (\theta^1 + y_O^1)|_{\xi=0+}$ . These expressions follow from the fact that  $\partial^2(\Theta^1 + F^1)/\partial \bar{\xi}^2 = \partial^2(\Theta^1 + O^1)/\partial \bar{\xi}^2 = 0$  (obtained by combining the equations above so as to eliminate the source terms) and the matching requirement with the outer solution which implies that  $\Theta^1 = \theta^1|_{\xi=0+}$ ,  $F^1 = y_F^1|_{\xi=0+}$  and  $O^1 = y_O^1|_{\xi=0+}$  as  $\bar{\xi} \rightarrow \infty$ .

Finally, the inner problem reduces to

$$\epsilon^2 (1 + f'^2) \frac{\partial^2 \Theta^1}{\partial \bar{\xi}^2} + \frac{1}{4} [(h^+ - \Theta^1)(k^+ - \Theta^1) - R] \exp \Theta^1 = 0, \tag{31}$$

subject to the matching conditions

$$\Theta^1 = \sigma + \bar{\xi} \left. \frac{\partial \theta^0}{\partial \xi} \right|_{\xi=0-} \quad \text{as} \quad \bar{\xi} \rightarrow -\infty \quad \text{and} \quad \Theta^1 = \sigma \quad \text{as} \quad \bar{\xi} \rightarrow \infty, \tag{32}$$

where  $\sigma \equiv \theta^1|_{\xi=0+}$  is the perturbation in the flame temperature. Now, on multiplying Equation (31) by  $\partial\Theta^1/\partial\xi$  and integrating with respect to  $\xi$  from  $\xi = -\infty$  to  $+\infty$  taking into account (32), we obtain

$$\begin{aligned}
 .2\epsilon^2(1 + f'^2)\left(\frac{\partial\theta^0}{\partial\xi}\right)^2|_{\xi=0-} &= \int_{-\infty}^{\sigma} [(h^+ - \Theta^1)(k^+ - \Theta^1) - R] \exp \Theta^1 d\Theta^1 \\
 &= (\sigma^2 - (h^+ + k^+ + 2)\sigma + h^+ + k^+ + h^+k^+ - R + 2) \exp \sigma,
 \end{aligned}
 \tag{33}$$

where the last expression is obtained on evaluating the integral.

The final step is to invoke chemical equilibrium behind the flame-front at  $\xi = 0+$ , which corresponds to setting the square bracket in the expression for  $\omega$  given in (15) to zero. This implies that  $y_F^1 y_O^1 - R = 0$ , i.e.

$$\sigma^2 - (h^+ + k^+)\sigma + h^+k^+ - R = 0
 \tag{34}$$

in terms of  $\sigma \equiv \theta^1|_{\xi=0+}$ ,  $h^+ \equiv (\theta^1 + y_F^1)|_{\xi=0+}$  and  $k^+ \equiv (\theta^1 + y_O^1)|_{\xi=0+}$ .

Equation (34) can be solved for  $\sigma$  to yield two real roots, the smaller of which, given by

$$\sigma = \frac{h^+ + k^+ - \sqrt{(h^+ - k^+)^2 + 4R}}{2},
 \tag{35}$$

is physically acceptable; the larger root is rejected since it leads to negative mass fractions as it implies that  $h^+ + k^+ - 2\sigma \leq 0$ , i.e.  $(y_F^1 + y_O^1)|_{\xi=0+} \leq 0$ .

The jump condition (28d) can now be easily obtained, after using (34) and (35) to simplify the r.h.s of (33), performing a few simple manipulations, and noting that  $\frac{\partial\theta^0}{\partial\xi}\Big|_{\xi=0+} = 0$  on account of  $\theta^0 = 1$  for  $\xi \geq 0$  and  $y \sim 1$ .

### 3.4. Small strain limit $\epsilon \ll 1$

In the  $\beta$ -free reformulated problem of Section 3.2, we now examine the small strain limit  $\epsilon \rightarrow 0$ . In this limit, the flame, including its preheat zone, can be viewed as an infinitely thin layer located at  $\xi = 0$ , since its thickness is  $O(\epsilon)$ . Outside this layer, diffusion and heat conduction can be neglected in a first approximation.

We shall write expansions in the form

$$f = f_0 + \epsilon f_1 + \dots, \quad U = U_0 + \epsilon U_1 + \dots$$

and similar expressions for  $\theta$ ,  $h$  and  $k$  written for the different regions. In particular, the local burning velocity  $S_L(y)$  defined by

$$S_L(y) \equiv \frac{U}{\sqrt{1 + f'^2}},
 \tag{36}$$

will have the expansion  $S_L = S_{L0}(y) + \epsilon S_{L1}(y) + \dots$  where

$$S_{L0} = \frac{U_0}{\sqrt{1 + f_0'^2}} \quad \text{and} \quad S_{L1} = \frac{1}{\sqrt{1 + f_0'^2}} \left[ U_1 - U_0 \frac{f_0' f_1'}{1 + f_0'^2} \right].
 \tag{37}$$

Similarly, the temperature of the flame-front,  $\theta_{Fl} \equiv \theta(\xi = 0^+, y)$ , will be expanded as

$$\theta_{Fl} = 1 + \frac{\sigma_0}{\beta} + \epsilon \frac{\sigma_1}{\beta} + \dots, \tag{38}$$

where  $\sigma$  is given by (35). Although expansion (38) will be determined explicitly later, we note here that its first term, equal to one, is the flame temperature of the planar stoichiometric flame under an irreversible reaction, its second term describes the deviation of the flame temperature from unity under infinitely weak strain ( $\epsilon = 0$ ) and should account for reversibility and the gradients of mass fractions far upstream given by (20), and its third term should account for the coupling between flame curvature, differential diffusion and reversibility.

### 3.4.1. Outer solution

On both sides of the flame,  $\xi < 0$  and  $\xi > 0$ , we seek outer expansions in the form

$$\theta^0 = \Theta_0 + \epsilon \Theta_1 + \dots, \quad h = H_0 + \epsilon H_1 + \dots, \quad k = K_0 + \epsilon K_1 + \dots$$

which we substitute into Equations (25)–(27). For  $\theta^0$  we find, taking into account the boundary conditions at  $\xi \rightarrow \pm\infty$ , that

$$\theta^0 = \Theta_0 = \begin{cases} 0 & \text{for } \xi < 0 \\ 1 & \text{for } \xi > 0, \end{cases} \quad \Theta_1 = \Theta_2 = \dots = 0. \tag{39}$$

We then find  $U_0 \partial H_0 / \partial \xi = U_0 \partial K_0 / \partial \xi = 0$ , which, when used with the upstream boundary conditions (29), implies that

$$H_0 = \begin{cases} -\gamma_F y & \text{for } \xi < 0 \\ A(y) & \text{for } \xi > 0 \end{cases} \tag{40}$$

and

$$K_0 = \begin{cases} \gamma_O y & \text{for } \xi < 0 \\ B(y) & \text{for } \xi > 0, \end{cases} \tag{41}$$

where  $A$  and  $B$  are integration constants which may depend on  $y$ .

### 3.4.2. Inner solution and results to leading order

Using the stretched variable  $\zeta \equiv \xi/\epsilon$ , we now examine the inner region of thickness  $O(\epsilon)$  around  $\xi = 0$  where diffusive effects should be retained. We introduce inner expansions in the form

$$\theta^0 = \theta_0 + \epsilon \theta_1 + \dots, \quad h = h_0 + \epsilon h_1 + \dots, \quad k = k_0 + \epsilon k_1 + \dots,$$

which when used in the jump conditions (3.2) yield, to leading order,

$$[\theta_0] = [h_0] = [k_0] = 0 \tag{42a}$$

$$\left[ \frac{\partial h_0}{\partial \zeta} \right] = -l_F \left[ \frac{\partial \theta_0}{\partial \zeta} \right] \quad (42b)$$

$$\left[ \frac{\partial k_0}{\partial \zeta} \right] = -l_O \left[ \frac{\partial \theta_0}{\partial \zeta} \right] \quad (42c)$$

$$\begin{aligned} \sqrt{1 + f_0'^2} \left[ \frac{\partial \theta_0}{\partial \zeta} \right] = & - \left( 1 + \frac{\sqrt{(h_0 - k_0)^2 + 4R}}{2} \right)^{1/2} \\ & \times \exp \left( \frac{h_0 + k_0 - \sqrt{(h_0 - k_0)^2 + 4R}}{4} \right). \end{aligned} \quad (42d)$$

In terms of  $\zeta$  the leading order equations in the inner region are

$$U_0 \frac{\partial \theta_0}{\partial \zeta} = (1 + f_0'^2) \frac{\partial^2 \theta_0}{\partial \zeta^2} \quad (43)$$

$$U_0 \frac{\partial h_0}{\partial \zeta} = (1 + f_0'^2) \frac{\partial^2 h_0}{\partial \zeta^2} + l_F (1 + f_0'^2) \frac{\partial^2 \theta_0}{\partial \zeta^2} \quad (44)$$

$$U_0 \frac{\partial k_0}{\partial \zeta} = (1 + f_0'^2) \frac{\partial^2 k_0}{\partial \zeta^2} + l_O (1 + f_0'^2) \frac{\partial^2 \theta_0}{\partial \zeta^2}. \quad (45)$$

These yield, when used together with the jump conditions (42a)–(42c) and matched with the outer solutions (39)–(41), the leading order solutions

$$\theta_0 = \begin{cases} \exp(\lambda \zeta) & \text{for } \zeta \leq 0 \\ 1 & \text{for } \zeta \geq 0 \end{cases} \quad (46)$$

$$h_0 = \begin{cases} -\gamma_F y - \lambda l_F \zeta \exp(\lambda \zeta) & \text{for } \zeta \leq 0 \\ -\gamma_F y & \text{for } \zeta \geq 0 \end{cases} \quad (47)$$

$$k_0 = \begin{cases} \gamma_O y - \lambda l_O \zeta \exp(\lambda \zeta) & \text{for } \zeta \leq 0 \\ \gamma_O y & \text{for } \zeta \geq 0 \end{cases} \quad (48)$$

where

$$\lambda \equiv \frac{U_0}{1 + f_0'^2}. \quad (49)$$

We note that in determining  $h_0$  and  $k_0$  for  $\zeta \geq 0$ , we have used the fact that no exponential growth as  $\zeta$  increases is allowed by matching; completing the matching allows the determination of  $A$  and  $B$  in (40) and (41), namely  $A = -\gamma_F y$  and  $B = \gamma_O y$ .

Using the remaining jump condition (42d) we obtain

$$S_{L0} = \left( 1 + \frac{\sqrt{(\gamma_F + \gamma_O)^2 y^2 + 4R}}{2} \right)^{1/2} \exp \left\{ \frac{(\gamma_O - \gamma_F)y - \sqrt{(\gamma_F + \gamma_O)^2 y^2 + 4R}}{4} \right\} \quad (50)$$

where  $S_{L0} \equiv U_0/(1 + f_0'^2)^{1/2}$  introduced in (37) is the local burning velocity, to leading order. The propagation speed  $U_0$  and the location of the leading edge,  $y^*$  say, can be determined from (50) using the fact that  $f_0' = 0$  and  $S'_{L0}(y) = 0$  at  $y = y^*$ . We thus find that

$$y^* = \frac{\gamma_O - \gamma_F}{2\gamma_F\gamma_O(\gamma_F + \gamma_O)} \left[ \gamma_F + \gamma_O + \sqrt{(\gamma_F - \gamma_O)^2 + 4\gamma_F\gamma_O R} \right] \quad (51)$$

and

$$U_0 = S_{L0}(y^*). \quad (52)$$

With  $S_{L0}$  and  $y^*$  being now known, the flame shape  $f_0(y)$  can be determined by integration using

$$f_0 = \int \left( \frac{S_{L0}^2(y^*)}{S_{L0}^2(y)} - 1 \right)^{1/2} dy. \quad (53)$$

We note that relations (50)–(53) can be expressed in terms of the stoichiometric coefficient  $S$  using (23); in particular, we find that

$$y^* = \frac{1 - S}{1 + S} \left( 1 + \frac{\sqrt{(1 - S)^2 + 4RS}}{1 + S} \right) \frac{\sqrt{\pi}}{2E} \quad (54)$$

and

$$U_0 = \frac{(1 + S)^{3/2}}{2S^{1/2}} \left( 1 + \frac{\sqrt{(1 - S)^2 + 4RS}}{1 + S} \right)^{1/2} \exp \left[ -\frac{\sqrt{(1 - S)^2 + 4RS}}{2(1 + S)} \right]. \quad (55)$$

From its definition,  $S \equiv s Y_{F,F} / Y_{O,O}$ , we have  $0 < S < \infty$ , with  $S = 1$  corresponding to a stoichiometric supply of reactants. In illustrating the results, however, only the range  $0 < S \leq 1$  needs be considered; indeed (50)–(53) imply that a change of  $S$  to  $S^{-1}$  changes the leading edge  $y^*$  to its negative and the graphs of  $f_0(y)$  and  $S_{L0}(y)$  to their symmetric with respect to the  $y = 0$  axis while keeping  $U_0$  unchanged, i.e.  $S \rightarrow S^{-1} \Rightarrow y^* \rightarrow -y^*$ ,  $f_0(y) \rightarrow f_0(-y)$ ,  $S_{L0}(y) \rightarrow S_{L0}(-y)$  and  $U_0 \rightarrow U_0$ . The last remark is expected from the definition of  $S$ , since changing  $S$  to  $S^{-1}$  is simply equivalent to swapping the ‘labels’ of the reactants as ‘Fuel’ and ‘Oxidizer’.

Figure 2 represents the local burning speed  $S_{L0}$  plotted against  $y$  for selected values of  $R$  and  $S$ . The top subfigure corresponds to the symmetric case of stoichiometric supply,  $S = 1$ , for which the peak of  $S_{L0}$  is located at  $y = 0$ ; here an increase in the reversibility parameter  $R$  is simply seen to decrease the burning speed and its peak, as expected. However, for  $S < 1$  as in the middle and bottom subfigures, we also see a shift in the peak location towards

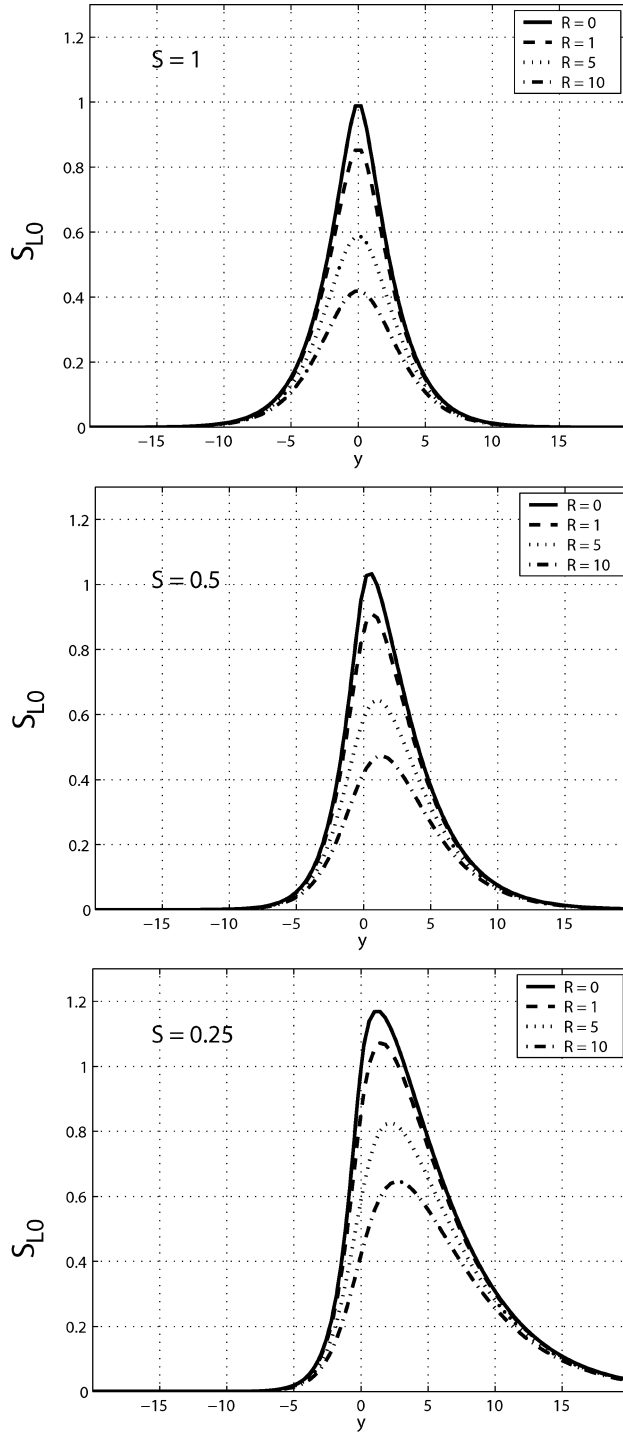


Figure 2. Local burning speed  $S_{L0}$  versus  $y$  for  $R = 0, 1, 5$  and  $10$ , and, from top to bottom,  $S = 1, 0.5$  and  $0.25$ .

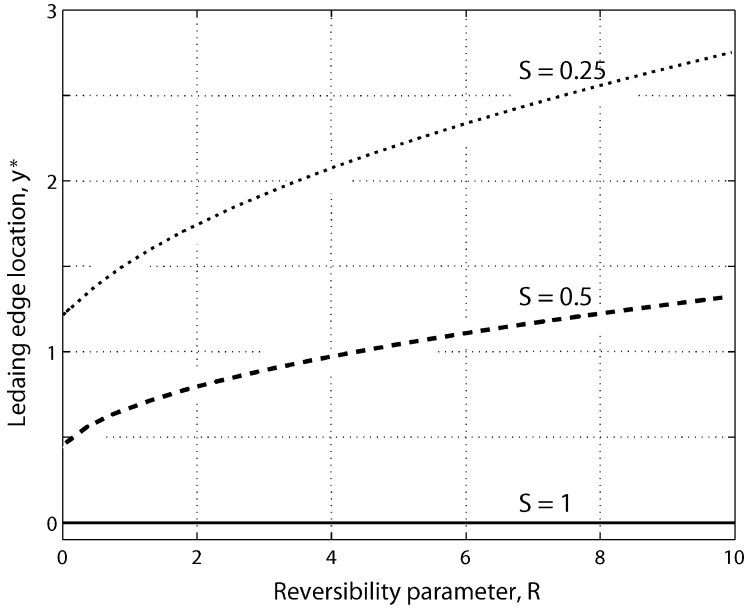


Figure 3. Leading edge location,  $y^*$ , versus  $R$ , for selected values of  $S$ .

$y = +\infty$  (the oxidizer side) as  $R$  is increased. These observations are further confirmed in Figures 3 and 4, where the location of the peak  $y^*$  and its amplitude  $U_0 = S_{L0}(y^*)$  are plotted versus  $R$  for selected values of  $S$ . The dependence of the flame shape  $x = f_0(y)$  on  $R$  and  $S$  is illustrated in Figure 5. We can again make the same remarks concerning the shift of the leading edge towards the oxidizer side as  $R$  is increased for  $S < 1$ . In addition,

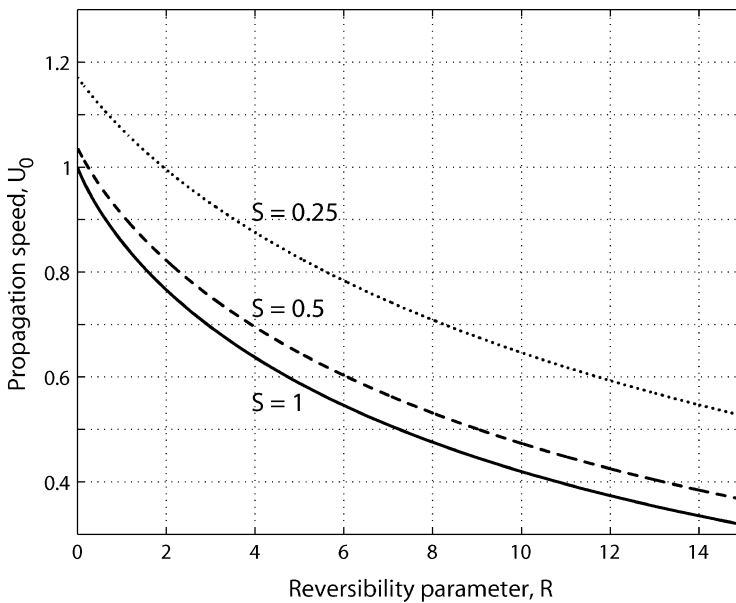


Figure 4. Leading order propagation speed,  $U_0$ , versus  $R$ , for selected values of  $S$ .

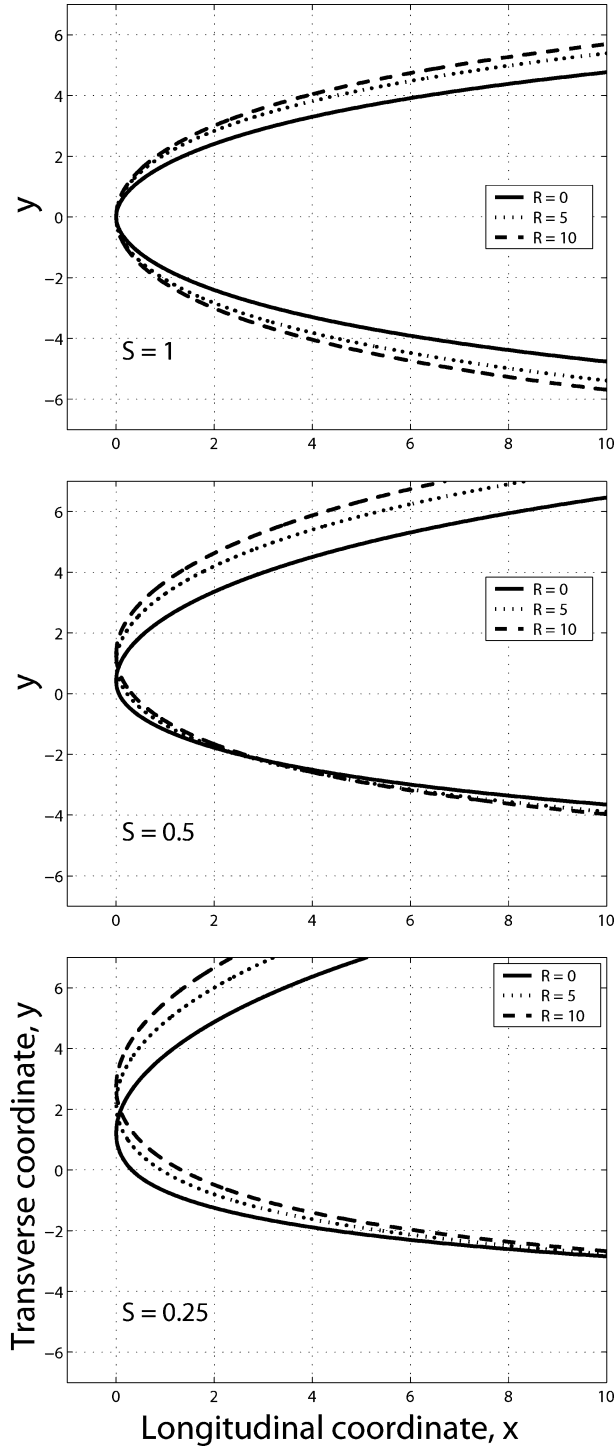


Figure 5. Flame shape,  $x = f_0(y)$ , for  $R = 0, 5$  and  $10$ , and, from top to bottom,  $S = 1, 0.5$  and  $0.25$ .

we note that an increase in  $R$  results in an decrease in the curvature of the flame-front which will naturally affect the burning speed in the next approximation addressed in the following section. At the leading edge, a simple formula for the flame curvature  $f_0''(y^*)$  can be derived, namely,

$$f_0''(y^*) = \sqrt{-\frac{S_{L0}''(y^*)}{S_{L0}(y^*)}}, \tag{56}$$

which follows from (53) and the fact that  $f_0'(y^*) = 0$  and  $S_{L0}'(y^*) = 0$ ; thus  $f_0''(y^*)$  can be evaluated from (50) and (51) although the resulting expressions are quite complex except in a few special cases including the stoichiometrically symmetric case  $S = 1$ , the irreversible case  $R = 0$ , and the case  $R = 1$ . For these special values of the parameters, for which the integrand of the square root in (54) and (55) is a complete square, simple expressions can be obtained on using (50), (54) and (56), namely,

$$y^* = 0 \quad \text{and} \quad f_0''(y^*) = \frac{\sqrt{2}}{\sqrt{\pi}(1 + \sqrt{R})^{\frac{1}{2}}} \quad \text{for} \quad S = 1, \tag{57}$$

$$y^* = \frac{1 - S}{1 + S} \left( 1 + \frac{|1 - S|}{1 + S} \right) \frac{\sqrt{\pi}}{2E} \quad \text{and} \quad f_0''(y^*) = \frac{1 + S}{S} \frac{E}{\sqrt{2\pi}} \quad \text{for} \quad R = 0, \tag{58}$$

and

$$y^* = \frac{1 - S}{1 + S} \frac{\sqrt{\pi}}{E} \quad \text{and} \quad f_0''(y^*) = \frac{1 + S}{\sqrt{1 + S^2}} \frac{E}{\sqrt{2\pi}} \quad \text{for} \quad R = 1, \tag{59}$$

where  $E$  is defined in (23). Such formulae, along with expression (55) for  $U_0$ , show the precise way in which the increase in  $R$  decreases the flame curvature and its propagation speed, to leading order.

The final point addressed in this section is the determination of the temperature  $\theta_{Fl}$  of the flame-front whose deviation from unity, to leading order, is determined by  $\sigma_0$ , in accordance with (38). The latter is in fact twice the argument of the exponential in (50), i.e.,

$$\sigma_0 = \frac{(\gamma_O - \gamma_F)y - \sqrt{(\gamma_F + \gamma_O)^2 y^2 + 4R}}{2}, \tag{60}$$

and its value at the leading edge,  $\sigma_0^*$  say, is twice the argument of the exponential in (55), i.e.,

$$\sigma_0^* = -\frac{\sqrt{(1 - S)^2 + 4RS}}{1 + S}. \tag{61}$$

Equation (60) implies that the maximum of  $\sigma_0$  and (hence of  $\theta_{Fl}$  to leading order) occurs at a location  $y_\theta^*$  which is related to the location of the leading edge  $y^*$  by

$$y_\theta^* = y^* \frac{2\sqrt{RS}}{1 + S + \sqrt{(1 - S)^2 + 4RS}}. \tag{62}$$

It follows that  $y_\theta^* = 0$  when  $R = 0$ , meaning that the maximum temperature of the triple-flame front (to leading order) occurs at the stoichiometric location  $y = 0$  in the irreversible case, irrespective of the location of the leading edge. This is not the case when the reaction is reversible however, since the maximum flame-front temperature is then sandwiched between the stoichiometric surface and the leading edge. Indeed, Equation (62) implies that  $0 \leq y_\theta^*/y^* \leq \sqrt{R}/(1 + \sqrt{R})$ , the upper bound which is clearly less than unity corresponding to the stoichiometrically symmetric case  $S = 1$ .

3.4.3. *Results in the next approximation*

In the previous section, a leading order description of the flame-front has been given, including the flame shape  $x = f(y)$ , the local burning speed  $S_L(y)$  and the propagation speed  $U$ . To obtain a better description, we carry out the asymptotic analysis to the next order in  $\epsilon$ .

If the operator  $L$  is defined by

$$L \equiv 2f_0'f_1' \frac{\partial^2}{\partial \zeta^2} - f_0'' \frac{\partial}{\partial \zeta} - 2f_0' \frac{\partial^2}{\partial y \partial \zeta}, \tag{63}$$

then the governing equations in the inner region are

$$\begin{aligned} U_0 \frac{\partial \theta_1}{\partial \zeta} - (1 + f_0'^2) \frac{\partial^2 \theta_1}{\partial \zeta^2} &= L(\theta_0) - U_1 \frac{\partial \theta_0}{\partial \zeta} \\ U_0 \frac{\partial h_1}{\partial \zeta} - (1 + f_0'^2) \frac{\partial^2 h_1}{\partial \zeta^2} &= L(h_0 + l_F \theta_0) - U_1 \frac{\partial h_0}{\partial \zeta} + l_F(1 + f_0'^2) \frac{\partial^2 \theta_1}{\partial \zeta^2} \\ U_0 \frac{\partial k_1}{\partial \zeta} - (1 + f_0'^2) \frac{\partial^2 k_1}{\partial \zeta^2} &= L(k_0 + l_O \theta_0) - U_1 \frac{\partial k_0}{\partial \zeta} + l_O(1 + f_0'^2) \frac{\partial^2 \theta_1}{\partial \zeta^2}. \end{aligned} \tag{64}$$

These are to be solved for  $\zeta \neq 0$ , subject to the jump conditions

$$\begin{aligned} [\theta_1] &= [h_1] = [k_1] = 0 \\ \left[ \frac{\partial h_1}{\partial \zeta} \right] &= -l_F \left[ \frac{\partial \theta_1}{\partial \zeta} \right] \\ \left[ \frac{\partial k_1}{\partial \zeta} \right] &= -l_O \left[ \frac{\partial \theta_1}{\partial \zeta} \right] \\ \left[ \frac{\partial \theta_1}{\partial \zeta} \right] &= \left( \frac{\sigma_1}{2} + \frac{(h_0 - k_0)(h_1 - k_1)}{2(h_0 - k_0)^2 + 8R + 4\sqrt{(h_0 - k_0)^2 + 4R}} - \frac{f_0'f_1'}{1 + f_0'^2} \right) \left[ \frac{\partial \theta_0}{\partial \zeta} \right] \end{aligned} \tag{65}$$

at the reaction sheet located at  $\zeta = 0$ . Here  $\sigma_1$  is the perturbation in the flame temperature given by

$$\sigma_1 = \frac{h_1 + k_1}{2} - \frac{(h_0 - k_0)(h_1 - k_1)}{2\sqrt{(h_0 - k_0)^2 + 4R}},$$

on account of (35). Downstream of the reaction sheet, it is found that  $\theta_1$  must be zero so as to be bounded as  $\zeta \rightarrow \infty$  and to match with (39). We thus have from (64) after eliminating

exponentially growing terms

$$\theta_1 = 0, \quad h_1 = \hat{h}_1, \quad k_1 = \hat{k}_1 \quad \text{for } \zeta \geq 0, \tag{66}$$

where  $\hat{h}_1$  and  $\hat{k}_1$  are independent of  $\zeta$  and are as yet undetermined.

Solving for  $\theta_1$  in the unburnt gas, it is found that

$$\theta_1 = \frac{\lambda}{U_0} \left[ U_1 - 2\lambda f_0' f_1' + f_0'' - 2 \frac{f_0'^2 f_0''}{1 + f_0'^2} \lambda \zeta \right] \zeta \exp(\lambda \zeta) \quad \text{for } \zeta \leq 0, \tag{67}$$

where  $\lambda$  has been defined in (49) and where use has been made of the matching requirement  $\theta_1 \rightarrow 0$  as  $\zeta \rightarrow -\infty$  and the continuity requirement  $\theta_1 = 0$  at  $\zeta = 0$ . We shall not need the explicit solutions for  $h_1$  and  $k_1$  below. We now integrate Equations (64) from  $\zeta = -\infty$  to  $\zeta = 0^-$  to obtain

$$\begin{aligned} (1 + f_0'^2) \left[ \frac{\partial \theta_1}{\partial \zeta} \right] &= I_\theta - U_1 \\ U_0 \hat{h}_1 &= I_h + l_F I_\theta \\ U_0 \hat{k}_1 &= I_k + l_O I_\theta, \end{aligned} \tag{68}$$

after using (47)–(48), (65)–(66), and the matching condition that  $\theta_1$ ,  $h_1$  and  $k_1$  and their derivatives with respect to  $\zeta$  must vanish as  $\zeta \rightarrow -\infty$ . In (68) we have introduced the quantities

$$I_\theta \equiv \int_{-\infty}^0 L(\theta_0) d\zeta, \quad I_h \equiv \int_{-\infty}^0 L(h_0) d\zeta, \quad \text{and} \quad I_k \equiv \int_{-\infty}^0 L(k_0) d\zeta$$

which can be evaluated from (46)–(48) and (67), to yield

$$I_\theta = 2 U_0 \frac{f_0' f_1'}{1 + f_0'^2} - f_0'', \quad I_h = -2 l_F U_0 \frac{f_0' f_1'}{1 + f_0'^2}, \quad I_k = -2 l_O U_0 \frac{f_0' f_1'}{1 + f_0'^2}.$$

When these expressions are used in (68), together with (47) and (65)–(67) we find

$$\begin{aligned} U_0 \hat{h}_1 &= -l_F f_0'' \\ U_0 \hat{k}_1 &= -l_O f_0'' \\ U_1 - \frac{U_0 f_0' f_1'}{1 + f_0'^2} &= -f_0'' + \frac{U_0 \sigma_1}{2} + \frac{U_0 (h_0 - k_0)(h_1 - k_1)}{2(h_0 - k_0)^2 + 8R + 4\sqrt{(h_0 - k_0)^2 + 4R}}. \end{aligned} \tag{69}$$

The system of equations (69) allows the determination of perturbation to the local burning velocity  $S_{L1}(y)$  introduced in (37). We thus find

$$S_{L1} = - \left( 1 + \frac{l_F + l_O}{4} + \frac{l_F - l_O}{4} \frac{(\gamma_O + \gamma_F)y}{2 + \sqrt{(\gamma_O + \gamma_F)^2 y^2 + 4R}} \right) \frac{f_0''}{(1 + f_0'^2)^{1/2}},$$

so that a two-term expansion of  $S_L$  in terms of  $\epsilon$  is now available, namely

$$S_L \sim S_{L0}(y) (1 - \tilde{L}(y)\kappa(y)) . \quad (70)$$

Here  $S_{L0}$  is determined by (50) and  $\kappa$  and  $\tilde{L}$  are given by

$$\kappa(y) = \frac{\epsilon}{S_{L0}(y)} \frac{f_0''}{(1 + f_0'^2)^{1/2}}, \quad (71)$$

$$\tilde{L}(y) = 1 + \frac{l_F + l_O}{4} + \frac{l_F - l_O}{4} \frac{(\gamma_O + \gamma_F)y}{2 + \sqrt{(\gamma_O + \gamma_F)^2 y^2 + 4R}} . \quad (72)$$

We note that  $\kappa$  and  $\tilde{L}$  appear as local non-dimensional *flame-stretch* and *Markstein length*, respectively. It is interesting to note that the Markstein length is affected by the reversibility parameter  $R$  and the local coordinate  $y$  whenever  $l_F \neq l_O$  and is independent of them otherwise.

For the perturbation in the propagation speed  $U_1$  we find

$$U_1 = -\tilde{L}(y^*) f_0''(y^*) \quad (73)$$

by applying Equations (69) at the leading edge  $y^*$  and using  $f_0'(y^*) = 0$ . In this expression, the Markstein length at the leading edge is given by

$$\tilde{L}(y^*) = 1 + \frac{l_F + l_O}{4} + \frac{l_F - l_O}{4} \frac{\gamma_O - \gamma_F}{\gamma_F + \gamma_O}$$

on using (51) and (72). This can be expressed in terms of the stoichiometric coefficient  $S$  as

$$\tilde{L}(y^*) = 1 + \frac{l_F + l_O}{4} + \frac{l_F - l_O}{4} \frac{1 - S}{1 + S},$$

on using (23). We note that the value of  $\tilde{L}$  at the leading edge  $y = y^*$  has turned out to be independent of  $R$ , which is not true for other values of  $y$ .

At this stage, a two-term approximation  $U \sim U_0 + \epsilon U_1$  is available from (52) and (73), namely,

$$U \sim S_{L0}(y^*) \left[ 1 - \frac{\epsilon}{S_{L0}(y^*)} \left( 1 + \frac{l_F + l_O}{4} + \frac{l_F - l_O}{4} \frac{1 - S}{1 + S} \right) \sqrt{-\frac{S_{L0}''(y^*)}{S_{L0}(y^*)}} \right], \quad (74)$$

where use has been made of (56), and where  $y^*$  and  $U_0 = S_{L0}(y^*)$  are to be evaluated from (54) and (55). This formula, which constitutes one of the main outcomes of the analysis, describes the dependence of the propagation speed  $U$  on the stoichiometric coefficient  $S$ , the reversibility parameter  $R$  and the reduced Lewis numbers  $l_F$  and  $l_O$ . In the particular case  $S = 1$ , it takes the simpler form

$$U \sim (1 + \sqrt{R})^{1/2} \exp \left( -\frac{\sqrt{R}}{2} \right) \left[ 1 - \left( 1 + \frac{l_F + l_O}{4} \right) \epsilon \sqrt{\frac{2}{\pi}} \frac{\exp(\sqrt{R}/2)}{1 + \sqrt{R}} \right], \quad (75)$$

after using (55) and (57). Likewise, a simple two-term expansion for  $U$  can be readily written down in the irreversible case  $R = 0$ , on using (55) and (58), which is more explicit than, but agrees with, a corresponding formula derived by Daou and Liñán [7].<sup>2</sup>

Similarly, we note for completeness that the results also allow the determination of a two-term expansion for the temperature of the flame-front  $\theta_{Fl}$  introduced in (38). It is found that

$$\begin{aligned} \theta_{Fl} &= 1 + \frac{\sigma_0}{\beta} + \epsilon \frac{\sigma_1}{\beta} + \dots \quad \text{with} \\ \sigma_0 &= \frac{(\gamma_O - \gamma_F)y - \sqrt{(\gamma_F + \gamma_O)^2 y^2 + 4R}}{2} \quad \text{and} \\ \sigma_1 &= - \left\{ \frac{l_F + l_O}{2} + \frac{l_F - l_O}{2} \frac{(\gamma_F + \gamma_O)y}{\sqrt{(\gamma_F + \gamma_O)^2 y^2 + 4R}} \right\} \frac{f_0''(y)}{U_0}, \end{aligned}$$

where  $\sigma_0$  has been determined using (60). The term in the rhs of this formula involving  $\sigma_0$  represents, as stated earlier, the deviation of the flame temperature from unity under infinitely weak strain ( $\epsilon = 0$ ) and the linear gradients of mass fractions far upstream given by (20). This deviation is seen to be a linear function of  $y$  only if  $R = 0$ , and its non-linearity when  $R \neq 0$  presents another characteristic of triple-flames attributable to the reversibility of the chemical reaction. The third term accounts for the coupling between flame curvature, differential diffusion and reversibility, and typically involves both Lewis numbers at any location  $y$  unless the reaction is irreversible; in the latter case only  $l_F$  is involved in the fuel-lean side  $y > 0$  and  $l_O$  in the oxygen-lean side  $y < 0$ . As a simple illustration in the particular case  $S = 1$ , the formula can be applied to show that the flame temperature *at the leading edge*,  $\theta_{Fl}^*$  say, is given by

$$\theta_{Fl}^* = 1 - \frac{\sqrt{R}}{\beta} - \frac{l_F + l_O}{2\beta} \epsilon \sqrt{\frac{2}{\pi}} \frac{\exp(\sqrt{R}/2)}{1 + \sqrt{R}}, \tag{76}$$

after using (57) and (61).

We close this section by a short discussion of the validity of the asymptotics, focusing attention on the asymptotic formula (75) for the propagation speed  $U$ . Shown in Figure 6 is a plot of  $U$  versus  $\epsilon$  based on this formula, for selected values of  $R$ ; for simplicity we set  $l_F = l_O = 0$  although the results are equally valid if the factor  $1 + (l_F + l_O)/4$ , assumed positive, is absorbed into  $\epsilon$ . The curves are straight lines whose ordinate at  $\epsilon = 0$ ,  $U_0$ , is a decreasing function of  $R$ , and their slope,  $U_1$ , is an increasing function of  $R$ . Any two such straight lines intersect thus each other, and the smallest value of  $\epsilon$  where a straight line pertaining to  $R \neq 0$  intersect other lines corresponds to the intersection point with the line  $R = 0$  of the irreversible case. The portion of the line beyond this smallest value of  $\epsilon$  is to be discarded, since the asymptotic formula is definitely invalid there since it predicts unexpected cases where the propagation speed increases with  $R$  for  $\epsilon$  fixed. These unexpected cases may be explained by the fact that, for fixed  $\epsilon$ , an increase in  $R$  promotes two effects which have opposing influences on  $U$ , namely a decrease in the flame-front curvature  $f_0''$  (see (57)) and a decrease in  $U_0$  (see (55)). These cases are however to

---

<sup>2</sup>For comparison sake, we mention that the parameter  $\Gamma$  in [7] is equal to  $S/(S + 1)$  and the parameter  $\Upsilon$  should be set to zero.

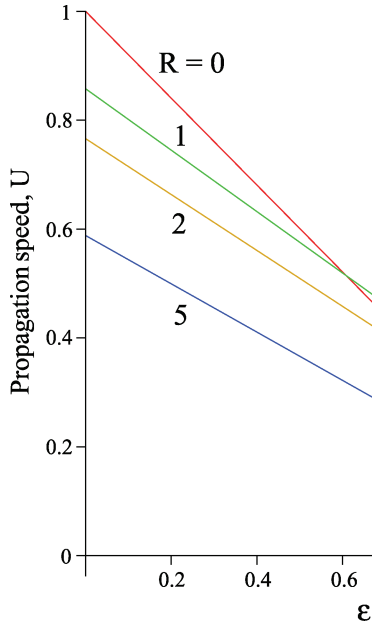


Figure 6. Propagation speed  $U$  versus  $\epsilon$  based on Equation (75), for selected values of  $R$ .

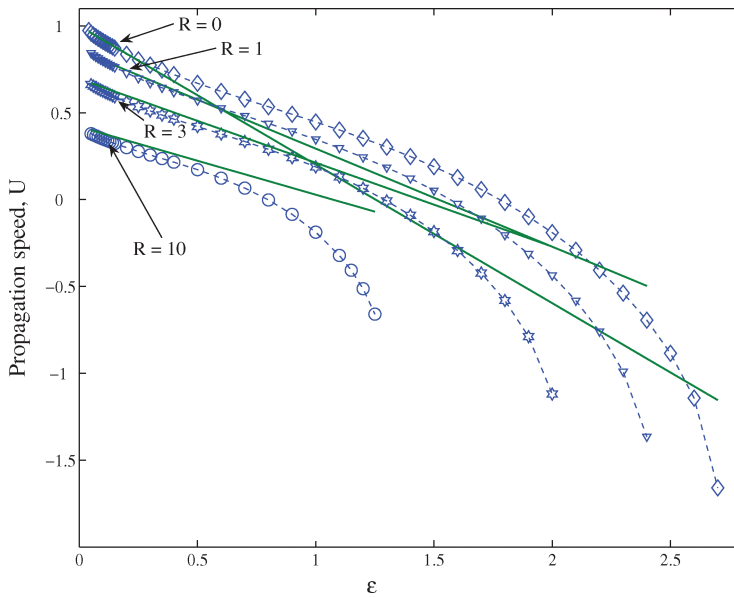


Figure 7. Propagation speed  $U$  versus  $\epsilon$  computed numerically (dashed lines) and based on the asymptotic formula (75) (solid lines), for selected values of  $R$ .

be rejected after comparison with extensive numerical results. A sample of the numerical results, obtained using the computational approach described in [7,22], is shown in Figure 7. Depicted in this figure is the propagation speed  $U$  versus  $\epsilon$  computed numerically<sup>3</sup> (dashed lines) and based on the asymptotic formula (75) (solid lines), for selected values of  $R$ . It is seen that the numerical results are in good agreement with the asymptotic predictions, and show that the latter have a rather wide range of validity.

#### 4. Conclusion

An asymptotic study of triple-flames in a strained mixing layer has been carried out under a reversible reaction. The investigation extends the analytical description of these flames beyond the common framework of a single irreversible Arrhenius reaction. The study identifies a suitable and physically motivated distinguished limit involving a specific scaling of the difference in the activation energies of the forward and backward reactions and of the degree of reversibility. Under this distinguished limit, which generalizes the classical near-equidiffusional-flame (NEF) approximation [32] to the reversible case, an extensive set of analytical results for weakly-strained triple-flames has been obtained. The results include the determination of the local burning speed, temperature and Markstein length along the flame-front, the shape, leading edge and curvature of the latter, and the propagation speed of the triple-flame. The formulae derived concisely account for the combined effect of several non-dimensional parameters characterizing the stoichiometry and reversibility of the chemical reaction, the strain rate, and the Lewis numbers of the reactants. In particular, it is found that the Markstein length is affected by the reversibility parameter and the local coordinate along the flame-front whenever the Lewis numbers of the fuel and oxidizer are unequal and is independent of them otherwise; in all cases however, it is value at the leading-edge which features in the explicit formula derived for the propagation speed  $U$  is found to be unaffected by the reversibility parameter. Several aspects specifically associated with the reversibility of the reaction are identified and quantified analytically, including the decrease in the propagation speed and flame-front curvature and the increased shift of the location of the leading edge away from the stoichiometric surface with increased reversibility. Some important features of triple-flames determined within a reversible reaction model are found to have no counterparts in the irreversible case. For example, whereas the maximum temperature of the triple-flame front occurs at the location of stoichiometric surface in the irreversible case, irrespective of the location of the leading edge, it is typically found to be sandwiched between these two locations in the reversible case, see (62).

Finally, we note that the findings and the methodology described can be seen as a first step towards accounting analytically for real chemistry effects on triple-flames, and towards modelling thin partially-premixed flames as propagating interfaces whose local burning speed is affected by the local composition gradients via a suitably defined local Markstein length.

---

<sup>3</sup>The numerical propagation speeds have been normalized (divided) by 0.75, which is the numerically determined burning speed of the irreversible stoichiometric *planar* flame with  $\beta = 8$ . The main reason for this normalization, which have been discussed and used in previous triple-flame studies, e.g. [7, 9, 22], is the fact that an infinite value of  $\beta$  is assumed in the asymptotics, while the value of  $\beta$  in the numerics is finite. This causes a common, rather trivial discrepancy between the laminar *planar* flame speeds computed numerically and asymptotically, which is most simply resolved by the normalization adopted, rather than by a computationally impractical increase in  $\beta$  to substantially higher values of the order of 30 (to achieve an agreement close to 5%, for small  $\epsilon$ ).

## References

- [1] H. Phillips, *Flame in a buoyant methane layer*, Tenth Symposium (International) on Combustion, The Combustion Institute (1965), pp. 1277–1283.
- [2] Y. Ohki and S. Tsuge, *Dynamics of reactive systems, Part I*, Bowen J.R., Leyer J.C. and Soloukhin R.I., eds., Prog. Astronautics and Aeronautics 105 (1986), p. 233.
- [3] J.W. Dold, *Flame propagation in a nonuniform mixture: Analysis of a slowly varying triple flame*, Combust. Flame 76 (1989), pp. 71–88.
- [4] L.J. Hartley and J.W. Dold, *Flame propagation in a nonuniform mixture: Analysis of a propagating triple-flame*, Combust. Sci. Technol. 80 (1991), pp. 23–46.
- [5] G.R. Ruetsch, L. Vervisch and A. Liñán, *Effects of heat release on triple flames*, Phys. Fluids 7(6) (1995), pp. 1447–1454.
- [6] J. Buckmaster and M. Matalon, *Anomalous Lewis number effects in tribrachial flames*, Twenty-second Symposium (International) on combustion, the Combustion Institute (1988), pp. 1527–1535.
- [7] J. Daou and A. Liñán, *The role of unequal diffusivities in ignition and extinction fronts in strained mixing layers*, Combust. Theory Model. 2 (1998), pp. 449–477.
- [8] R. Daou, J. Daou and J. Dold, *Effect of volumetric heat loss on triple-flame propagation*, Proc. Combust. Inst. 29 (2002), pp. 1559–1564.
- [9] R. Daou, J. Daou and J. Dold, *The effect of heat loss on flame edges in a non-premixed counterflow within a thermo-diffusive model*, Combust. Theory Model. 8 (2004), pp. 683–699.
- [10] V. Kurdyumov and M. Matalon, *Radiation losses as a driving mechanism for flame oscillations*, Proc. Combust. Inst. 29 (2002), pp. 45–52.
- [11] M.S. Cha and P.D. Ronney, *Propagation rates of nonpremixed edge flames*, Combust. Flame 146 (2006), pp. 312–328.
- [12] J. Buckmaster, *Edge-flames*, Prog. Energy Combust. Sci. 28 (2002), pp. 435–475.
- [13] V. Kurdyumov and M. Matalon, *Dynamics of an edge-flame in a mixing layer*, Combust. Flame 139 (2004), pp. 329–339.
- [14] V. Kurdyumov and M. Matalon, *Stabilization and onset of oscillation of an edge-flame in the near-wake of a fuel injector*, Proc. Combust. Inst. 31 (2007), pp. 909–917.
- [15] A. Liñán, in *Combustion in High Speed Flows*, J. Buckmaster, T.L. Jackson, and A. Kumar, eds., Kluwer Academic, Boston, 1994, p. 461.
- [16] P.N. Kioni, B. Rogg, K.N.C. Bray and A. Liñán, *Flame spread in laminar mixing layers: the triple flame*, Combust. Flame 95 (1993), pp. 276–290.
- [17] P.N. Kioni, K.N.C. Bray, D.A. Greenhalgh and B. Rogg, *Experimental and numerical studies of a triple flame*, Combust. Flame 116 (1999), pp. 192–206.
- [18] T. Plessing, P. Terhoeven, N. Peters and M.S. Mansour, *An experimental and numerical study of a laminar triple flame*, Combust. Flame 115 (1998), pp. 335–353.
- [19] T. Echekki and J.H. Chen, *The effects of complex chemistry on triple flames*, in *Studying Turbulence Using Numerical Databases*, Vol. VI, CTR, Stanford, 1996, pp. 217–234.
- [20] H.G. Im and J.H. Chen, *Structure and propagation of methanol–air triple flames*, Combust. Flame 114 (1998), pp. 231–245.
- [21] H.G. Im and J.H. Chen, *Structure and propagation of triple flames in partially premixed hydrogen–air mixtures*, Combust. Flame 119 (1999), pp. 436–454.
- [22] S. Ali and J. Daou, *Effect of the reversibility of the chemical reaction on triple flames*, Proc. Combust. Inst. 31 (2007), pp. 919–927.
- [23] Ya.B. Zeldovich, H.I. Barrenblatt, V.B. Librovich, and G.M. Makhviladze, *The Mathematical Theory of Combustion and Explosions*, Consultants Bureau, New York, 1985.
- [24] J.F. Clarke, *Reaction-broadening in a hydrogen–oxygen diffusion flame*, Proc. Roy. Soc. A 312 (1969), pp. 65–83.
- [25] F. Fendell, *Combustion in initially unmixed reactants for one-step reversible chemical kinetics*, Astronaut. Acta. 13 (1967), pp. 183–191.
- [26] F. Fendell, *Flame structure in initially unmixed reactants for one-step kinetics*, Chem. Engng Sci. 22 (1967) pp. 1829–1837.
- [27] J. Daou, P. Haldenwang and C. Nicoli, *Supercritical burning of liquid oxygen (LOX) droplet with detailed chemistry*, Combust. Flame 101 (1995), pp. 153–169.
- [28] N. Peters, *Premixed burning in diffusion flames – The flame zone model of Libby and Economos*, Int. J. Heat Transf. 22 (1979), pp. 691–703.

- [29] A. Bonnet, *Travelling-wave solutions to combustion models for a reversible reaction*, SIAM J. Math. Anal. 27 (1996), pp. 1270–1285.
- [30] A.P. Aludushin, B.J. Matkowsky and V.A. Volpert, *Stoichiometric flames and their stability*, Combust. Flame 101 (1995), pp. 15–25.
- [31] J. Daou, *Premixed flames with a reversible reaction: Propagation and stability*, Combust. Theory Model. 12 (2008), pp. 349–365.
- [32] J.D. Buckmaster and G.S.S. Ludford, *Lectures on Mathematical Combustion*, Society for Industrial and Applied Mathematics, Philadelphia, 1983.
- [33] G. Joulin and P. Vidal, *Hydrodynamics and Nonlinear Instabilities*, Cambridge University, Cambridge, 1998.